Anisotropic Magnetic Exchange observed by Electron Spin Resonance in Hexaammineruthenium(III) Chloride Sulfate Trihydrate†

Philip A. Reynolds,* Lutz M. Engelhardt and Alexander N. Sobolev
Department of Chemistry, University of Western Australia, Nedlands, W.A. 6009, Australia

The orthorhombic crystal structures of $[M^{III}(NH_3)_6]Cl[SO_4]\cdot 3H_2O$ for M = Ru at 295 K and M = Ru or Co at 92 K have been determined by X-ray diffraction. Single-crystal ESR experiments on a ruthenium doped cobalt crystal at 77 K are interpreted simply in terms of a *g* tensor with principal values 2.005(6), 2.123(4) and 1.629(4) aligned almost along the *a*, *b* and *c* axes. This can be parameterised by a crystal-field model, and its orientation understood in terms of the crystal structure. However the pure ruthenium salt, unlike the ruthenium doped cobalt salt, shows unusual structure in its ESR spectra. The structure is extremely broad in energy, comparable with the microwave energy, but with a number of distinct peaks in the resonance which change dramatically with crystal orientation. The broadened spectra result from magnetic exchange between nearest neighbours occupying a two-dimensional network in the crystal. Since the exchange energies are greater than differences in single-ion energy terms, it is only the anisotropy in the magnetic exchange that is observed. It has principal values −0.18(2), 0.070(2) and 0.102(3) cm^{-1} (or all signs reversed), with principal axes approximately along *a*, *b* and *c*. It is highly unusual to observe structure due to such large magnetic exchange in ESR studies of magnetically concentrated materials.

We have begun a study of the magnetic properties of various hexaammineruthenium(III) salts. The aim is to calculate these very variable properties directly from the structure by *ab initio* methods for several crystals. Ultimately we wish to avoid the use of empirical, hard to interpret, crystal-field models, even though such models can provide excellent fits to data with good observable/parameter ratios. This would incorporate magnetic properties into the list of properties routinely calculable for transition-metal compounds by rigorous quantum mechanical methods.

Hexaammineruthenium(III) salts have been selected for the initial data gathering because large single crystals can often be obtained. These contain the cation in a wide variety of torsional conformations and crystal environments.[1–3] Magnetic exchange may be small and the single-ion magnetic properties are very variable and highly anisotropic. This variability results from different crystal fields acting on an orbitally degenerate low-spin d^5 ion in which there is significant spin–orbit coupling. Small magnetic exchange permits useful ESR experiments in magnetically concentrated salts. We must use pure crystals if we are to start our calculations with a definite cation geometry, not the guessed geometry of a magnetic defect in a magnetically diluted crystal.

Our first experiments were on $[Ru(NH_3)_6]Br[SO_4]$[4] and $[Ru(NH_3)_6][SCN]_3$[5] mainly by single-crystal ESR spectroscopy and SQUID magnetic measurements. These could be explained by crystal-field models in which the number of empirical parameters is well outweighed by the amount of experimental data. This result, rarely shown for low-symmetry crystals, enables us to proceed in similar crystals by using only the often easier technique of ESR spectroscopy to determine the magnetic properties.

The ESR resonances in these two crystals, while somewhat broadened by the small magnetic exchange present, were unstructured and relatively narrow. They had a typical width of 20–30 mT at the resonant centre field of *ca.* 450 mT. However, when we examined the ESR spectra of single crystals of $[Ru(NH_3)_6]Cl(SO_4]\cdot 3H_2O$ we observed highly structured spectra between 0 and 900 mT. Moreover these changed dramatically with crystal orientation.

Structure, associated with magnetic exchange, has been previously observed in magnetically concentrated transition-metal compounds.[6–11] However in these cases the structure extended over only a few tens of mT. In this case, where, if the structuring is due to exchange, the microwave and exchange energies are comparable, then simple theory suggests that structured ESR resonances should not be observable. In such situations a single broad resonance is observed, and exchange information is obtained from lineshape and width, not from structure.[12–14] The large-scale structure observed here in a magnetically concentrated material is, we believe, highly unusual, and may not have been observed before.

Nevertheless we shall show below, by reference to single-crystal ESR spectroscopy and X-ray diffraction experiments on ruthenium, cobalt and ruthenium doped cobalt crystals of $[M^{III}(NH_3)_6]Cl[SO_4]\cdot 3H_2O$, that the structure is due to magnetic exchange coupling; and that information about its anisotropy can be obtained from this ESR data.

Experimental

Preparations.—The compound $[Ru(NH_3)_6]Cl[SO_4]\cdot 3H_2O$ was prepared by addition of an excess of an equimolar mixture of ammonium chloride and sulfate to an aqueous solution of hexaammineruthenium(III) chloride, followed by evaporation. It was recrystallised from water by slow evaporation to give large honey-coloured truncated octahedra. Pure cobalt(III) hexaammine chloride sulfate trihydrate, and cobalt hexaammine crystals doped with *ca.* 1% ruthenium(III), were prepared in the same way and gave dark amber truncated octahedra.

Structure Determinations.—We have determined the structure of $[Ru^{III}(NH_3)_6]Cl[SO_4]\cdot 3H_2O$ at 295 and 92 K and that of

---

† *Supplementary data available:* see Instructions for Authors, *J. Chem. Soc., Dalton Trans.*, 1994, Issue 1, pp. xxiii–xxviii.

$[Co^{III}(NH_3)_6]Cl[SO_4]\cdot 3H_2O$ at 92 K by X-ray diffraction. The experimental and refinement details are given in Table 1.

The structures were solved by direct methods followed by use of Fourier difference maps to locate missing atoms. Reflections with $I > 3\sigma(I)$ were used in the refinement of positional and thermal parameters by full-matrix least-squares refinement on $||F_o| - |F_c||$. Hydrogen positional parameters were not refined for the 92 K ruthenium crystal structure. All atom thermal parameters, except hydrogen, were anisotropic. Hydrogen thermal parameters were refined isotropically, except for the ruthenium structure at 92 K where they were set at 1.2 times that of the bonded atom. Neutral-atom form factors with dispersion corrections were used,[15] computation used the SHELX 92 program system.[16] Extinction was significant but not critical in all three cases, the maximum reduction in intensity was never more than 20% for any reflection. Atomic coordinates, equivalent thermal parameters and bond lengths and angles are given in Tables 2 and 3.

Additional material available from the Cambridge Crystallographic Data Centre comprises thermal parameters and remaining bond lengths and angles.

The cell contents excluding hydrogens projected onto the *ab* and *bc* planes are shown in Fig. 1(*a*) and (*b*) respectively for the 295 K ruthenium structure. One of the four short Ru ••• Ru contacts (at 681 pm) is indicated. Fig. 2 shows the geometry of

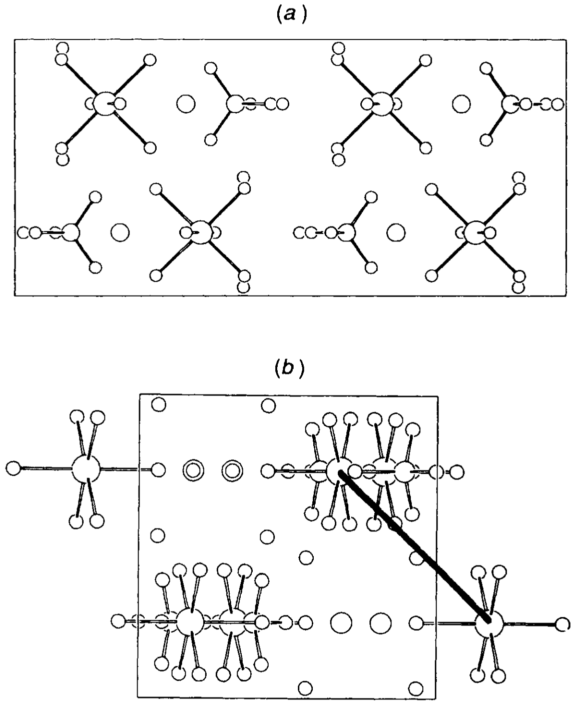

Fig. 1 The unit cell with hydrogens omitted in (*a*) *ab* (*a* horizontal) and (*b*) *bc* projection (*c* horizontal)

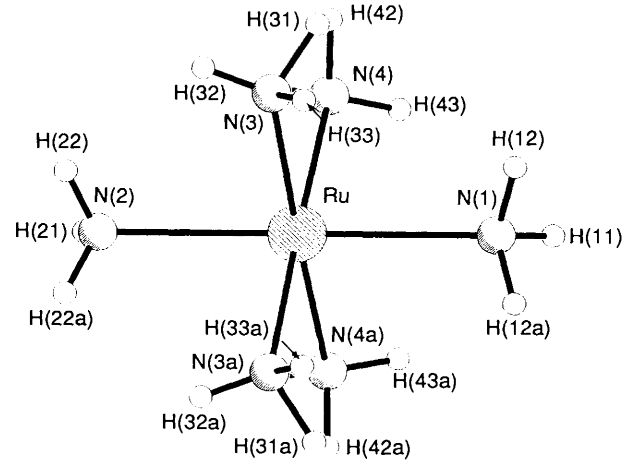

Fig. 2 The geometry of the $Ru(NH_3)_6$ fragment, *ac* projection

Table 1 Experimental details and refinement of structure determinations *

Compound	$[Ru(NH_3)_6]Cl[SO_4]\cdot 3H_2O$	$[Ru(NH_3)_6]Cl[SO_4]\cdot 3H_2O$	$[Co(NH_3)_6]Cl[SO_4]\cdot 3H_2O$
T/K	295	92	92
M_r	388.8	388.8	346.6
Machine	Enraf–Nonius CAD-4	Nicolet P3	Nicolet P3
F(000)	796	796	730
a/pm	1823.6(3)	1831.3(8)	1801.3(8)
b/pm	866.2(1)	864.3(4)	850.2(4)
c/pm	846.9(1)	829.4(3)	834.4(3)
U/nm^3	1.338(1)	1.313(2)	1.278(2)
D_m/Mg m^{-3}	1.91(2)	—	—
D_c/Mg m^{-3}	1.93	1.97	1.80
μ-Mo/mm^{-1}	1.53	1.56	1.74
Maximum dimension/mm	0.25	0.3	0.2
Total data	3574	2234	2817
Unique data	3574	2234	1992
Observed data [$I > 3\sigma(I)$]	2499	1812	1652
Maximum 2θ/°	75	60	60
Range *h*, *k*, *l*	0–31, 0–14, 0–10	−4 to 25, −2 to 11, −11 to 4	−4 to 25, −2 to 11, −11 to 4
Analytical absorption (max., min.)	Not applied	0.61, 0.66	0.70, 0.76
No. of standards	6	6	6
Decay of standards	0.02	0.05	0.05
$10^4 a$	3	22	5
No. of parameters	138	138	138
R	0.030	0.036	0.023
R′	0.034	0.037	0.025
Goodness of fit	0.69	0.92	1.07
Max., min. electron density in difference map/e nm^{-3}	1100, −800	1900, −3800	500, −900

* Details in common: orthorhombic, space group *Pnma*; $Z = 4$; morphology, {011} and {100}, subsidiary faces {201} and {210}; weighting scheme $w = 1/[\sigma^2(F) + aF^2]$.

Table 2 Positional (× 10^4, × 10^3 for H) and isotropic thermal parameters (10^{-1} pm^2 for non-H atoms, 10^{-2} pm^2 for H atoms) for $[Ru(NH_3)_6]Cl[SO_4]\cdot 3H_2O$ at 295 K (first entry) and 92 K (second entry) and for $[Co(NH_3)_6]Cl[SO_4]\cdot 3H_2O$ at 92 K (third entry) *

Atom	*x*	*y*	*z*	U_{iso}
Ru	3357(1)	2500	3226(1)	15(2)
Ru	3335(1)	2500	3344(1)	7(1)
Co	3332(1)	2500	3280(1)	6(1)
N(1)	3616(2)	2500	5650(4)	34(2)
N(1)	3560(2)	2500	5841(3)	14(1)
N(1)	3568(1)	2500	5587(2)	11(1)
N(2)	3097(2)	2500	800(3)	25(2)
N(2)	3098(2)	2500	957(3)	11(1)
N(2)	3092(1)	2500	976(3)	10(1)
N(3)	4152(1)	784(2)	2910(3)	25(2)
N(3)	4138(1)	782(2)	3054(2)	11(1)
N(3)	4091(1)	868(2)	2986(2)	10(1)
N(4)	2552(1)	805(2)	3602(3)	24(2)
N(4)	2529(1)	796(2)	3698(2)	10(1)
N(4)	2569(1)	887(2)	3632(2)	9(1)
Cl	1905(1)	2500	6842(1)	32(2)
Cl	1871(1)	2500	6983(1)	12(1)
Cl	1887(1)	2500	6946(1)	11(1)
S	1009(1)	2500	1087(1)	20(2)
S	1018(1)	2500	1226(1)	9(1)
S	1003(1)	2500	1180(1)	7(1)
O(1)	369(1)	2500	23(4)	46(2)
O(1)	360(1)	2500	174(3)	16(1)
O(1)	335(1)	2500	144(2)	15(1)
O(2)	729(2)	2500	2728(3)	33(2)
O(2)	765(1)	2500	2929(3)	14(1)
O(2)	753(1)	2500	2882(2)	13(1)
O(3)	1459(1)	1113(2)	827(2)	33(2)
O(3)	1459(1)	1093(2)	923(2)	14(1)
O(3)	1453(1)	1078(1)	875(1)	12(1)
O(1w)	152(2)	2500	−3181(6)	36(2)
O(1w)	137(1)	2500	−3103(3)	15(1)
O(1w)	131(1)	2500	−3103(2)	15(1)
O(2w)	870(1)	−333(3)	4343(3)	39(2)
O(2w)	853(1)	−356(2)	4464(2)	16(1)
O(2w)	877(1)	−366(2)	4449(2)	16(1)
H(11)	333(3)	250	637(7)	2(1)
H(11)	308	250	638	2
H(11)	319(2)	250	615(4)	2(1)
H(12)	386(2)	167(5)	586(5)	5(1)
H(12)	380	172	608	2
H(12)	379(1)	173(3)	592(3)	3(1)
H(21)	263(4)	250	64(6)	5(2)
H(21)	255	250	70	2
H(21)	259(2)	250	83(4)	4(1)
H(22)	328(2)	174(5)	39(5)	4(1)
H(22)	330	160	34	3
H(22)	330(1)	173(3)	53(3)	2(1)
H(31)	408(3)	−8(5)	343(4)	5(1)
H(31)	397	4	359	3
H(31)	397(1)	4(3)	355(3)	2(1)
H(32)	421(3)	50(7)	207(7)	7(2)
H(32)	417	53	208	3
H(32)	415(1)	55(3)	200(3)	2(1)
H(33)	458(4)	87(8)	330(5)	7(2)
H(33)	451	109	343	3
H(33)	451(1)	119(3)	336(3)	3(1)
H(41)	224(2)	71(4)	285(4)	2(1)
H(41)	225	81	287	2
H(41)	224(1)	85(3)	286(3)	3(1)
H(42)	275(2)	−11(5)	360(5)	4(1)
H(42)	275	−11	360	2
H(42)	275(1)	−2(3)	370(3)	2(1)
H(43)	229(2)	100(5)	447(5)	6(1)
H(43)	230	103	455	4
H(43)	232(1)	111(3)	454(3)	2(1)
H(11w)	22(5)	250	−260(9)	3(1)
H(11w)	11	250	−213	2
H(11w)	54(4)	250	−225(5)	4(1)
H(12w)	54(2)	250	−366(7)	5(1)
H(12w)	59	250	−358	6
H(12w)	50(2)	250	−348(5)	4(1)
H(21w)	54(2)	−91(6)	409(5)	5(1)
H(21w)	53	−83	406	3
H(21w)	56(1)	−89(3)	408(3)	3(1)
H(22w)	84(2)	43(5)	393(5)	5(1)
H(22w)	84	46	394	3
H(22w)	84(1)	43(3)	398(3)	3(1)

* For non-H atoms equivalent isotropic *U* defined as one third of the trace of the orthogonalised U_{ij} tensor. For the structure of $[Ru(NH_3)_6]Cl[SO_4]\cdot 3H_2O$ at 92 K the H-atom parameters were constrained and the positional parameters, located by Fourier difference maps, were not refined.

the hexaammineruthenium(III) ion, projected onto the *ac* plane. In Table 4 we list one of each pair (related by mirror in *b*) of Ru ··· Ru contacts < 1200 pm, representing a total of only 16 contacts, many symmetry related. In Table 5 we list the hydrogen-bonded contacts with X ··· H less than 260 pm.

Electron Spin Resonance Studies.—A Bruker ER 100 spectrometer with a liquid-nitrogen Dewar for sample cooling was used at X-band frequency. Scans from indicated 0 to 900 mT were made. No correction for the residual magnetisation of *ca.* 5 mT of the poles was made. Single crystals were mounted using Apiezon grease on a flat surface perpendicular to the applied magnetic field. The flat surface was machined in a Perspex rod mounted vertically. The rod was attached to a rotating angular scale. The crystal and rod were immersed in liquid nitrogen. The whole assembly is capable of aligning the crystal to within 2° with respect to the magnetic field. The pure crystals of $[Ru(NH_3)_6]Cl[SO_4]\cdot 3H_2O$ were aligned using an optical goniometer, after preliminary examination under a polarising microscope. The ruthenium doped hexaammine cobalt crystals, because *b* and *c* are very similar, retained an ambiguity in alignment. This was resolved by comparison of derived *g* values for pure and doped materials.

Resonances were observed at 15° rotation intervals for the hexaammine ruthenium crystals in the *ab*, *bc* and *ac* planes, and in ruthenium doped hexaammine cobalt crystals in planes *ac* and *bc*. Examples are illustrated in Fig. 3.

In the doped material, as expected from the crystal structure, single resonances were observed with the magnetic field in the *ac* plane and two resonances in the *bc* plane which coalesce with the field along *b* or *c*. The unit cell contains two pairs of magnetically equivalent ions. Each *g* tensor is constrained, by crystal symmetry, to have a principal axis parallel to *b*. The absorptions were narrow, less than 10 mT, enabling easy determination of the resonant fields. The rotation curve in *bc* was fitted to the two principal *g* parameters and the angle of the principal axes with respect to the crystal axes. The results are shown in Table 6. The resonances showed poorly resolved nuclear fine structure. Ruthenium contains 80% of isotopes with nuclear spin $I = 0$, and 20% with $I = \frac{5}{2}$. The latter in $[Ru(NH_3)_6]Cl_3$ give A_i values varying from 41(2) × 10^4 to 54(2) × 10^{-4} cm.[17] We observe here an average *A* of 50(4) × 10^{-4} cm^{-1}.

In the pure crystal we see structured resonances extending over 4–500 mT (Fig. 3). They are highly dependent on crystal orientation. This unusual behaviour in pure paramagnetic

Table 3 Non-hydrogen bond distances (pm) and angles (°), for $[M(NH_3)_6]Cl[SO_4]\cdot 3H_2O$ (M = Ru or Co)

	M = Ru, 295 K	M = Ru, 92 K	M = Co, 92 K
M–N(1)	210.7(3)	211.2(2)	197.1(2)
M–N(2)	210.9(3)	210.8(3)	197.1(2)
M–N(3)	209.5(2)	210.4(2)	196.3(2)
M–N(4)	210.0(2)	210.6(2)	196.4(2)
S–O(1)	147.3(3)	148.7(2)	148.2(2)
S–O(2)	148.2(3)	148.6(2)	149.0(2)
S–O(3)	147.0(2)	148.2(2)	147.7(1)
N(1)–M–N(2)	180.0(2)	179.4(2)	179.7(1)
N(1)–M–N(3)	88.2(1)	88.6(1)	88.4(1)
N(2)–M–N(3)	91.8(1)	91.8(1)	91.8(1)
N(1)–M–N(4)	90.5(1)	90.0(1)	90.2(1)
N(2)–M–N(4)	89.5(1)	89.6(1)	89.6(1)
N(3)–M–N(4)	90.4(1)	90.7(1)	90.7(1)
N(3)–M–N(3a)	90.4(1)	89.8(1)	90.0(1)
N(4)–M–N(3a)	178.5(1)	178.5(1)	178.5(1)
N(4)–M–N(4a)	88.8(1)	88.8(1)	88.6(1)
O(1)–S–O(2)	107.5(1)	107.8(1)	108.1(1)
O(1)–S–O(3)	110.4(1)	110.0(1)	110.2(1)
O(2)–S–O(3)	109.4(1)	109.3(1)	109.3(1)
O(3)–S–O(3a)	109.6(1)	110.3(1)	109.9(1)

Table 4 Separations between the Ru ion at 0.3357, 0.25, 0.6774 and Ru ions with the indicated positional parameters (at 92 K)

Separation/pm	*x*	*y*	*z*
681	0.1643	−0.25	0.1774
681	0.1643	−0.25	1.1774
798	0.6643	−0.25	0.3226
846	0.3357	0.25	1.6774
866	0.3357	1.25	0.6774
919	0.6643	−0.25	1.3276
920	0.8357	0.25	0.8226
1163	0.8357	0.25	−0.1774

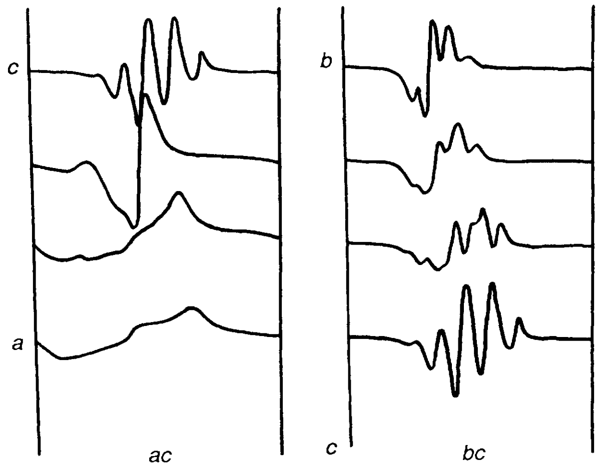

Fig. 3 ESR resonances observed in crystals of $[Ru(NH_3)_6]Cl[SO_4]\cdot 3H_2O$. The width displayed is from 0 to 900 mT. Spectra are shown at 30° intervals for rotation in the *ac* and *bc* planes from 0 to 90°

Table 5 Hydrogen bond contacts (lengths in pm, angles in °) in $[Ru(NH_3)_6]Cl[SO_4]\cdot 3H_2O$ at 295 K

O(1) ··· H(33)	247	O(2w) ··· H(22)	217
O(2) ··· H(22w)	207	O(2w) ··· H(32)	232
O(3) ··· H(12)	247	Cl ··· H(42)	263
O(3) ··· H(31)	241	Cl ··· H(43)	253
O(1w) ··· H(21w)	200	Cl ··· H(11w)	253

O(1) ··· H(33) ··· N(3)	143
O(2) ··· H(22w) ··· O(2w)	176
O(3) ··· H(12) ··· N(1)	135
O(3) ··· H(31) ··· N(3)	144
O(1w) ··· H(21w) ··· O(2w)	171
O(2w) ··· H(22) ··· N(2)	158
O(2w) ··· H(32) ··· N(3)	161
Cl ··· H(42) ··· N(4)	145
Cl ··· H(43) ··· N(4)	155
Cl ··· H(11w) ··· O(1w)	141

Table 6 Principal *g* values and angles (°) with respect to crystal axes of an Ru^{III} doped crystal of $[Co(NH_3)_6]Cl[SO_4]\cdot 3H_2O$

	g_1	g_2	g_3
	1.629(4)	2.005(6)	2.123(4)
Angles with			
a	93(1)	3(1)	90
b	90	90	0
c	3(1)	93(1)	90

crystals of transition-metal complexes will be discussed below. Here we note that amongst other regularities, all the spectra are almost symmetric about a particular field. This suggests that we are observing not-so-fine structure on a normal resonance. These centre fields can be fitted with $g_a = 2.00(8)$, $g_b = 2.216(7)$, $g_c = 1.604(8)$. These values are very similar to the values obtained in the doped crystal, but the differences are significant. The error in g_a is large because the resonance is extremely broad. The intensity of the resonance also decreases as the magnetic field approaches *a*.

The pure powder ESR spectrum is apparently, and misleadingly, a very broadened single resonance with little structure.

Crystal Field Modelling.—A rhombic crystal-field model with a general orientation in the crystal has been shown to be an excellent model for describing the single-crystal magnetic, ESR and spectroscopic properties of $[Ru(NH_3)_6][SCN]_3$.[5] We will use the same model here on $[Ru(NH_3)_6]Cl[SO_4]\cdot 3H_2O$.

Such a crystal-field model for the $^2T_{2g}$ state of a Ru^{III} ion on a site of mirror crystallographic symmetry requires eight parameters. Five of these parameters, *viz.* $10Dq$, interelectronic repulsions F_2 and F_4, the spin–orbit coupling constant ζ, and the Stevens orbital reduction factor k, we would expect to be transferrable between hexaammineruthenium(III) salts. As for the tristhiocyanate salt we restrict the basis to t_{2g} orbitals, removing the need for $10Dq$, F_2 and F_4, since these have little effect on the final result; ζ we set at 1000 cm^{-1} and k at 0.94, as is found to be satisfactory for other hexaammineruthenium(III) salts. We fix the crystal field orientation at the experimental orientation. We then require values for two further parameters, the energies of $3d_{xz}$ and $3d_{yz}$ relative to $3d_{xy}$. These may be obtained by fitting the three observed principal *g* values. Use of $3d_{xz}$ at -235 cm^{-1} and $3d_{yz}$ at -125 cm^{-1} gives $g_x = g_a = 1.951$, $g_y = g_b = 2.211$ and $g_z = g_c = 1.603$. These are in good agreement with the values for the pure salt.

We note again here that the ESR results alone only just determine the required parameters. However in the similar case of the tristhiocyanate addition of substantial extra single crystal magnetisation data did not change the crystal field parameters.

Spin–orbit coupling is calculated to split the $^2T_{2g}$ state into three Kramers doublets. The ground state is separated by 1454 cm^{-1} from the first excited state when there is no applied magnetic field.

Discussion

Structure.—The structure of $[Ru(NH_3)_6]Cl[SO_4]\cdot 3H_2O$ consists of water, hexaammineruthenium(III), sulfate and chloride fragments linked by X–H ··· Y bonds. Table 5 shows that no atom or fragment is bonded insufficiently that disorder or abnormal thermal motion might result.

In Fig. 2 we see that the $Ru(NH_3)_6$ fragments has almost *mm* symmetry and that there is no approximate centre of inversion. In addition to the crystallographically required mirror plane in the plane of the figure, there is almost a mirror plane in the *ab* plane, that is vertical in the figure. The N(1) and N(2) atoms of two of the ammonia molecules are in the crystallographic *ac* mirror plane. Given the approximate three-fold rotational symmetry, and absence of inversion symmetry, this produces an approximate mirror plane in the *ab* planes as well. The approximate three-fold symmetry of the N(4) and N(3) ammonias ensures that they will have *ab* mirror symmetry for dihedral angles of 0 and 0°. At 92 K for the Ru salt we observe −1.4 and −26.9°, not far from the values required for overall *mm* fragment symmetry.

If we turn to the bonding to the rest of the crystal of the $Ru(NH_3)_6$ fragment, we see far less symmetry. The N(1) and N(2) ammonias are both bonded through the two out-of-plane hydrogens, with a bent bond, but the distances are quite dissimilar, 247 and 217 pm respectively. The N(3) hydrogens are more evenly bonded with three bonds from 232 to 247 pm to sulfate oxygens. Atom N(4) has only two bonds, both to Cl, from H(42) and H(43). Overall the hydrogen bonds conform rather less well to *mm* symmetry than the $Ru(NH_3)_6$ fragment itself.

The rest of the crystal bonding is unexceptional. We have a short, almost linear, water–water hydrogen bond of O(1w) ··· H(21w) with a distance of 200 pm. This produces a hydrogen bonded cluster of three water molecules. The other shorter hydrogen bond is from water to sulfate, O(2) ··· H(22w) of 207 pm. O(1) and O(3) are hydrogen bonded to ammine hydrogens at longer distances. This difference in hydrogen bonding may be the reason why the S–O(2) bond is distinctly longer than the S–O(1) and S–O(3) bonds in two of the three structures.

The ruthenium–ruthenium distances are sparsely distributed. There are only four contacts under 800 pm. These four are all symmetry related by a mirror plane in *b* and/or a two-fold screw-axis along *c*.

Magnetic Properties.—(*a*) *Hamiltonian and ESR considerations.* We write the spin Hamiltonian in the usual way as the sum of single-ion and magnetic exchange terms, equation (1).

$$H = \sum_i H_i + \sum_{ij} H_{ij} \qquad (1)$$

For the single-ion term we have the magnetic field and nuclear hyperfine terms, equation (2) and the magnetic exchange Hamiltonian term can be expressed by equation (3),

$$H_i = \beta \boldsymbol{H} \cdot \boldsymbol{g} \cdot \boldsymbol{S}_i + \boldsymbol{S}_i \cdot \boldsymbol{A} \cdot \boldsymbol{I}_i \qquad (2)$$

$$H_{ij} = J\boldsymbol{S}_i \cdot \boldsymbol{S}_j + \boldsymbol{S}_i \cdot \boldsymbol{J'}_{ij} \cdot \boldsymbol{S}_j + \boldsymbol{D}_{ij} \cdot \boldsymbol{S}_i \times \boldsymbol{S}_j \qquad (3)$$

where J is the scalar isotropic exchange term; $\boldsymbol{J'}_{ij}$ the symmetric anisotropic term—a symmetric traceless tensor; and $\boldsymbol{D}_{ij}$ is the antisymmetric anisotropic Dzialoshinski–Moriya term, a polar vector (or when rearranged an antisymmetric tensor with zero diagonal elements). This accounts for the nine possible elements in the general tensor interaction.

Theory for weakly interacting dimers shows two contrasting cases.[18] Where single-ion energy terms are large compared to magnetic exchange, ESR spectroscopy can measure the total magnetic exchange. However when single ion energies are small compared with magnetic exchange, ESR will measure only the anisotropy in the magnetic exchange. ESR experiment[6] has demonstrated both cases, measuring either isotropic exchange or the anisotropy of the exchange for appropriate systems.

In the same way we expect two limiting cases for undiluted paramagnetic crystals. Experimentally only the situation with large single-ion energy terms has been observed. Where nuclear hyperfine energies are large compared with exchange, the structure observed in the ESR spectra over some tens of mT can be fitted with single ion terms, an isotropic magnetic exchange parameter, and calculated dipole–dipole interionic magnetic interactions (*e.g.* refs. 9 and 10). However where exchange is large compared with single ion terms, there are generally so many different interionic terms, particularly dipole–dipole, that only a single very broad unstructured resonance is observed.

To observe highly structured ESR resonances due to magnetic anisotropy requires further favourable circumstances. First, that for different ions, the single-ion energies should be closely similar. Ideally this means all ions are magnetically equivalent, and with the same g tensor, and that there is no nuclear fine structure because $I_i = 0$. Secondly that the magnetic centres are well separated in the crystal, so that dipolar broadening is minimised. Thirdly that, even though the magnetic centres are well separated, which reduces magnetic exchange overall, sufficient anisotropy in this exchange must still occur. Such anisotropy arises from spin–orbit coupling. Ideally we require a second- or third-row transition metal, to obtain a high spin–orbit coupling constant, with plenty of orbital moment as well. Finally the anisotropy of the magnetic exchange should be similar for all magnetically inequivalent metal–metal interactions; *i.e.* all magnetic 'bonds' should have the *same* anisotropy, not just symmetry related anisotropy. As we shall see all four of these conditions are met quite well in this present experiment.

(*b*) *Single ion properties.* The g tensor is found to be aligned almost coincident with the *abc* coordinate system. We have noted that the $Ru(NH_3)_6$ fragment has approximate *mm* symmetry in this axis system, while the bonding arrangement of this cation to the rest of the crystal does not. We can infer that the g-tensor orientation is governed more by the local symmetry of the ammine hydrogens, than by more distant interactions. However since the ammine torsional angles are themselves determined by the rest of the crystal,[3] the rest of the crystal does have an indirect effect, mediated through the ammines.

The 'accidental' close alignment of the g tensor with *abc* means that the two magnetically inequivalent sites in the crystal have almost identical g-tensor alignments, differing in orientation by only 6(2)°. Together with the 80% $I_i = 0$ isotope mixture in natural ruthenium, this means that energy differences between various ions in the crystal are much smaller than is usual.

(*c*) *Magnetic exchange.* When Ru^{III} is doped into the isomorphous cobalt hexaammine salt we see relatively narrow resonances, with some nuclear hyperfine structure from the $I = \frac{5}{2}$ ruthenium isotope. In the pure ruthenium hexaammine salt these resonances are broadened by several hundred mT. Dipolar fields are small. We calculated maxima of 5.9, 5.9, 3.7, 3.1, 2.9, 2.4, 2.4 and 1.2 mT per ion for the eight nearest-neighbour pairs of ions. Given these small values, dipolar effects cannot account for this broadening. The source of this structured, symmetrical, broadening is magnetic exchange interaction with neighbouring ions.

There are only four nearest neighbours at a relatively long distance of 681 pm. We may thus expect quite small nearest-neighbour magnetic exchange, of a two-dimensional nature in the *bc* plane. Other neighbours are few, and significantly more distant, with, we might expect, negligible magnetic exchange.

However the four magnetic interactions are not equivalent. The off-diagonal elements of the exchange anisotropy tensor change sign among the four interactions. Initially, working in the *abc* coordinate system, we will assume these terms are negligible. For the Dzialoshinski–Moriya term there is the further consideration that spin canting in this system, calculated from the crystal-field model, never exceeds thirty degrees for any magnetic field. Thus the $\boldsymbol{S}_i \times \boldsymbol{S}_j$ term is generally much smaller than $\boldsymbol{S}_i \cdot \boldsymbol{S}_j$, reducing the effect of this term in the Hamiltonian.

We will proceed on the assumption that the structure of the ESR spectra is caused by magnetic exchange with only the four nearest neighbours, and that the interactions with these neighbours are effectively magnetically equivalent with the principal axes *abc*.

When the magnetic field is applied along *a*, *b* and *c* directions there will be no spin canting because the *g* tensor has almost these three principal axes. So we will be measuring the diagonal components of the anisotropic exchange tensor. Any off-diagonal components will not contribute under those conditions. With four magnetically equivalent neighbours we may expect five resonances at energies of $g\beta H - \frac{3}{2}J'$, $g\beta H - \frac{3}{4}J'$, $g\beta H$, $g\beta H + \frac{3}{4}J'$ and $g\beta H + \frac{3}{2}J'$ and with intensities in the ratio 1:4:6:4:1 if the temperature is high compared with the isotropic part of the magnetic exchange.[18]

With the field along *b* and *c* there are clearly five resonances, with intensities consistent with such a binomial distribution. From these we can estimate $J'_{bb} = \pm 75(2)$ mT and $J'_{cc} = \pm 109(3)$ mT. Since there is a smooth passage from one to the other as we rotate about *a*, we can assign the same sign to J'_{bb} and J'_{cc}. The term J'_{bb} is the element of the symmetric anisotropic magnetic exchange term, $\boldsymbol{J}_{ij}$, connecting the spin components along the *b* crystal direction of nearest ruthenium neighbours; J'_{aa},J'_{ac} *etc.* are defined similarly.

When the magnetic field is along *a* the resonance is broad, and the structure is much less obvious. However one can still assign three resonances, with $J'_{aa} = \mp 200(20)$ mT. The outermost pair of resonances, weak in the *b* and *c* spectra are not visible here. We have assigned the sign of J'_{aa} opposite to that of J'_{bb} and J'_{cc}, because when we rotate the magnetic field direction towards *c* from *a* or *b*, the resonances collapse rapidly. At about 30° from *a* or *b* we have something resembling a single broad resonance. This suggests that the exchange anisotropy passes through zero, changing sign between *a* and *c* field directions. We note that the sum rule applicable for a traceless tensor, $J'_{aa} + J_{bb} + J'_{cc} = 0$, is also satisfied by this assignment.

The fact that a five-line spectrum can explain our spectra so well supports our assignment of *abc* as the approximate principal axes of the anisotropy tensor and neglect of the Dzialoshinski–Moriya terms. However at *ca.* 45° from *b* and *c* the resonances at $g\beta H \pm \frac{3}{4}J'$ are apparently split into two, while the other three are apparently unsplit. This is a reflection that we actually have two inequivalent pairs of ions magnetically coupled to the central ion, not four equivalent. Off-diagonal elements of the magnetic exchange tensor are not negligible. In such a situation the outermost pair of resonances will be unsplit, the next split equally into two equal resonances, and the central resonance into three of relative intensity 1:4:1. With resonances of the width here the minor splitting of the central peak may remain unnoticed, but that of the next, being an equal splitting may not. The difference in the two J' values appears to maximise at *ca.* one third of the mean J'. This gives a rough estimate of $|J'_{bc}|$ as about 30 mT. Examination of the exchange pathway and relative ionic orientations may enable us to understand such differences. When the field is parallel to *b* or *c* it is at about 45° to all four nearest neighbour Ru–Ru vectors. Conversely, when the field is midway between *b* and *c* it is, almost, perpendicular to one pair of exchange pathways and parallel to the other pair. Naively this is when we might expect differences in 'bond' properties, such as magnetic exchange will be maximised.

We have identified four of the nine components of the magnetic exchange $J'_{aa} = -0.18(2)$, $J'_{bb} = 0.070(2)$, $J'_{cc} = 0.102(3)$ (or all with opposite sign), and $|J'_{bc}| = 0.02(1)$ cm^{-1}. Effects from the other two off-diagonal elements, and the Dzialoshinski–Moriya term have not been detected, and may be smaller.

The occurrence of spin canting for magnetic fields not along *a*, *b* or *c* complicates simulations of these spectra. However, given more detailed experimental ESR data, simulation may become worthwhile. In particular lower temperatures, use of both X- and Q-band radiation, and use of intermediate ruthenium dilutions may be useful. Measurement of the magnetic susceptibilities, fixing the isotropic magnetic exchange component and giving confirmatory anisotropy information, would also be worthwile.

Acknowledgements

The authors are indebted to the Australian Research Council for financial support both directly and through Professor B. N. Figgis and Dr. G. S. Chandler. P. A. R. wishes to acknowledge support from an ARC Fellowship.

References

1 K. Gleu, W. Cuntze and K. Rehm, *Z. Anorg. Allg. Chem.*, 1938, **237**, 89.
2 K. Gleu and K. Rehm, *Z. Anorg. Allg. Chem.*, 1936, **227**, 237.
3 L. M. Engelhardt, P. A. Reynolds and A. N. Sobolev, *Aust. J. Chem.*, in the press.
4 P. A. Reynolds, C. D. Delfs, B. N. Figgis, L. M. Engelhardt, B. Moubaraki and K. S. Murray, *J. Chem. Soc., Dalton Trans.*, 1992, 2029.
5 A. B. Blake, C. D. Delfs, L. M. Engelhardt, B. N. Figgis, P. A. Reynolds, B. Moubaraki and K. S. Murray, *J. Chem. Soc., Dalton Trans.*, 1993, 1417.
6 C. P. Keijzers, *Electron Spin Resonance*, Specialist Periodical Report, Royal Society of Chemistry, London, 1987, vol. 10B, p. 1.
7 G. D. Simpson, R. L. Belford and R. Biagioni, *Inorg. Chem.*, 1978, **17**, 2424.
8 K. W. Plumlee, B. M. Hoffman, J. A. Ibers and Z. G. Soos, *J. Chem. Phys.*, 1975, **63**, 1926.
9 B. Gahan and F. E. Mabbs, *J. Chem. Soc., Dalton Trans.*, 1983, 1695.
10 D. Collison, B. Gahan and F. E. Mabbs, *J. Chem. Soc., Dalton Trans.*, 1983, 1705.
11 H. So, G. P. Haightard and R. L. Belford, *J. Phys. Chem.*, 1980, **84**, 1849.
12 P. T. Manoharan, *Proc. Indian Acad. Sci. Sect. A*, 1986, **52**, 715.
13 A. Bencini and D. Gatteschi, *EPR of Exchange Coupled Systems*, Springer Verlag, Berlin, 1990.
14 R. D. Willett, *Magnetostructural correlations in exchange coupled systems*, eds. R. D. Willett, D. Gatteschi and O. Kahn, D. Reidel, Dordrecht, 1985, p. 297.
15 J. A. Ibers and W. C. Hamilton (Editors), *International Tables for X-Ray Crystallography*, Kynoch Press, Birmingham, 1974, vol. 4.
16 G. A. Sheldrick, *J. Appl. Crystallogr.*, in the press.
17 J. H. E. Griffiths, J. Owen and I. M. Ward, *Proc. R. Soc. London*, 1953, **219**, 526.
18 A. Abragam and B. Bleaney, *Electron Paramagnetic Resonance of Transition Ions*, Oxford University Press, Oxford, 1970, pp. 491–529.

Received 4th *August* 1993; *Paper* 3/04702D